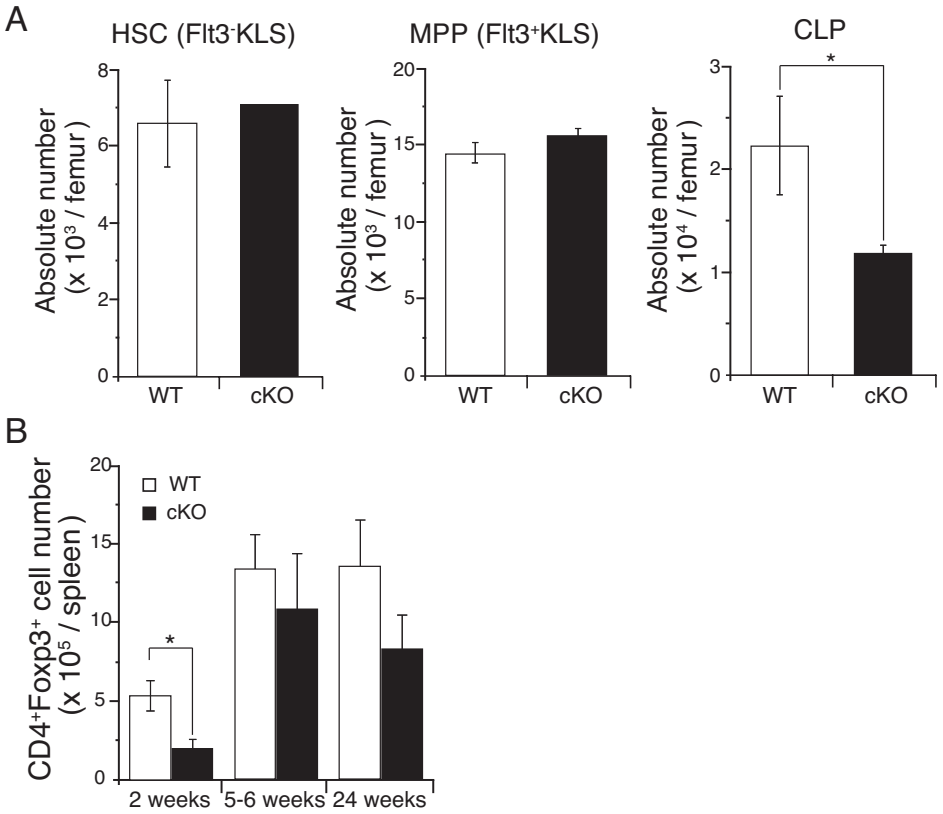

Supplemental Figure 1. (**A**) T cell development was arrested at the CLP stage in BM in the absence of SATB1. The number of HSC ($Flt3^{-}c\text{-}Kit^{hi}Lin^{-}Sca\text{-}I^{+}$ cells), MPP ($Flt3^{+}c\text{-}Kit^{hi}Lin^{-}Sca\text{-}I^{+}$ cells) and CLP ($IL\text{-}7R\alpha^{+}c\text{-}Kit^{lo}Lin^{-}Sca\text{-}I^{lo}$ cells) cells in the bone marrow from one femur of a WT (open bars, n=3) or a SATB1cKO (closed bars, n=3) mouse is shown. Student's *t*-test was used for statistical analysis (*p<0.05). (**B**) Treg cell numbers in the spleen of WT (open bars, n=5) and SATB1cKO mice (closed bars) at different ages (*p<0.05).

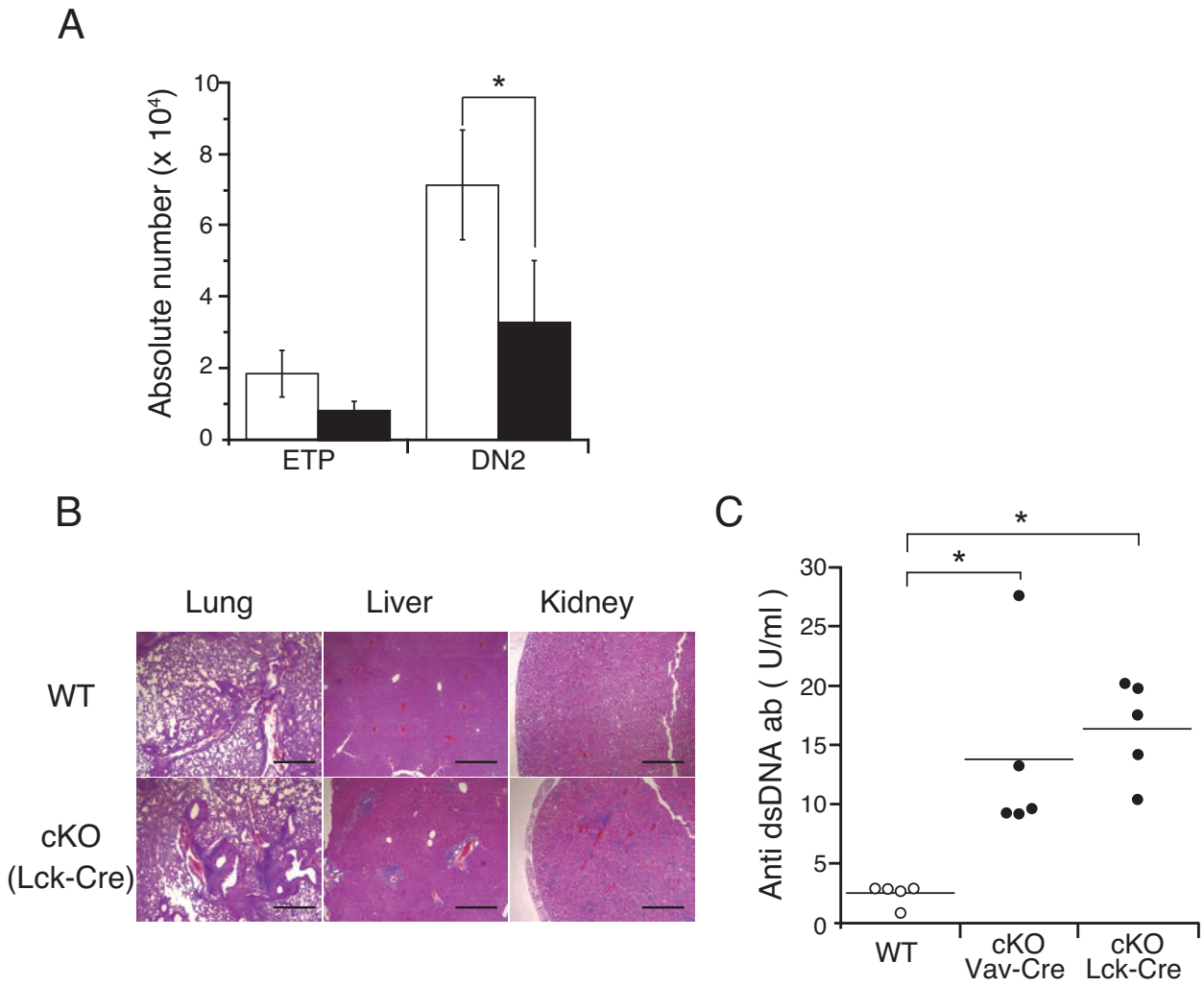

Supplemental Figure 2. Autoimmune disorders occur in *Lck*-Cre SATB1$^{fl/fl}$ mice. (**A**) The number of ETP (c-Kit^{+}CD25^{-}CD44^{+} DN) or the DN2 (c-Kit^{+}CD25^{+}CD44^{+} DN) fraction of thymocytes in WT mice (open bars, n=5) and in SATB1$^{fl/fl}$ mice with *Lck*-Cre transgenes (closed bars, n=5) is shown (*p<0.05). (**B**) H&E staining of sections of various organs from WT and *Lck*-Cre SATB1$^{fl/fl}$ mice. (**C**) Concentration of anti-dsDNA antibodies in the serum of WT, *Vav*-Cre SATB1$^{fl/fl}$ and *Lck*-Cre SATB1$^{fl/fl}$ mice.

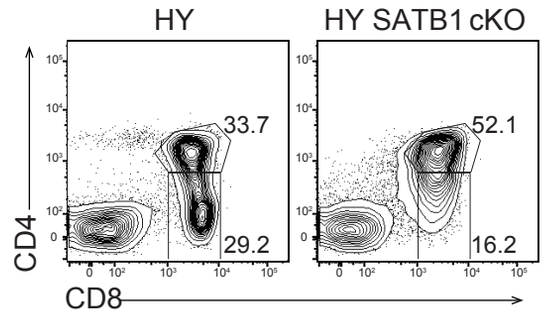

Supplemental Figure 3. Transition from a DP to a CD8$^+$ SP population is perturbed in female HY-TCR$^+$ mice on a SATB1 cKO background. Expression of CD4 and CD8 on HY-TCR-expressing T3.70$^+$ thymocytes from female HY-TCR TG mice on a WT (left) or a SATB1cKO background (right) was analyzed on FACS. Representative results from more than 5 analyses are shown.

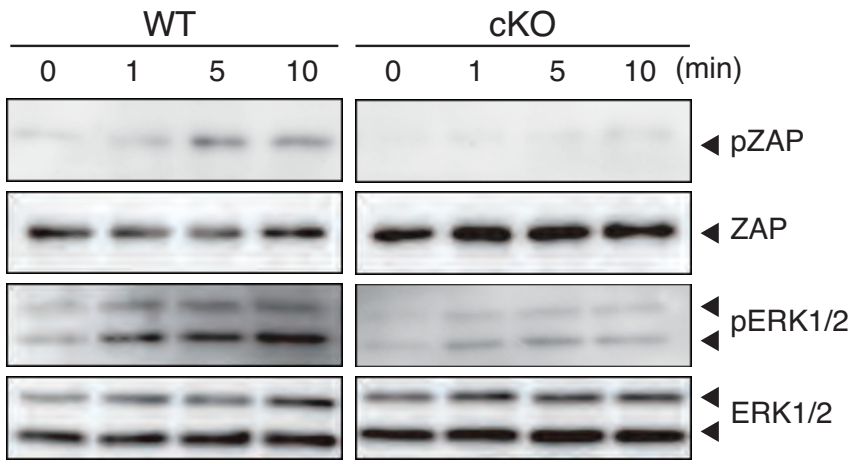

Supplemental Figure 4. Signal strength via TCR is weak in T cells from SATB1cKO mice. Naïve $CD4^+$ T cells were purified from the spleen of WT and SATB1cKO mice and stimulated with anti-CD3 and anti-CD28 antibodies for indicated periods. Whole cell lysates were subjected to SDS-page. Separated proteins were transferred to PVDF membrane, which was blotted with antibodies indicated in the figure.